Exoplanets: History

First extrasolar planet discovery (2 planets orbiting a pulsar PSRB1257+12):
Wolszczan & Frail, 1992, Nature, 355, 145

First exoplanet around a MS star – 51 Peg:
Mayor & Queloz, 1995, Nature, 378, 355

First transiting exoplanet - HD 209458b:
Henry et al. 2000, ApJ 529, L41, Charbonneau et al. 2000, ApJ 529, L45

Two Earth-sized transiting planets (orbiting Kepler 20):
Fressin et al. 2012, Nature, 482, 195
A 2.4 Re planet in the habitable zone of a Sun-like star (Kepler-22b):
Borucki et al. 2012, ApJ, 745, 1208

Exoasteroids WD1145+017: Vanderburg et al. 2015
Exocomets KIC 3542116: Rappaport et al. 2018

as of Mar 10, 2022: 4983 confirmed exoplanets (3515 transiting, 994 rad.vel., 187 imaging, 173 microlensing, timing 47)

Corot, Kepler, TESS, JWST...

COROT (convection, rotation and planetary transits).

- (CNES, European mission)
- Launched in Dec.27, 2006, decommissioned in 2013.
- 27cm telescope, will monitor about 120 000 stars
- Observing runs 20-150 days in one field.
- COROT is most sensitive to the orbits with periods of 50 days or less.
- 2.8x2.8deg field of view.
- It has a prism to separate the colors. Camera operating in the visible.
- Camera sensitive to changes in a star's light of just one part in 100 000
- 3-colour light curves thanks to a prism mounted in front of the exoplanet channel camera detectors (CCD's) made it possible to distinguish between the different families of detected events (transits, stellar activity, eclipsing binaries).

WISE

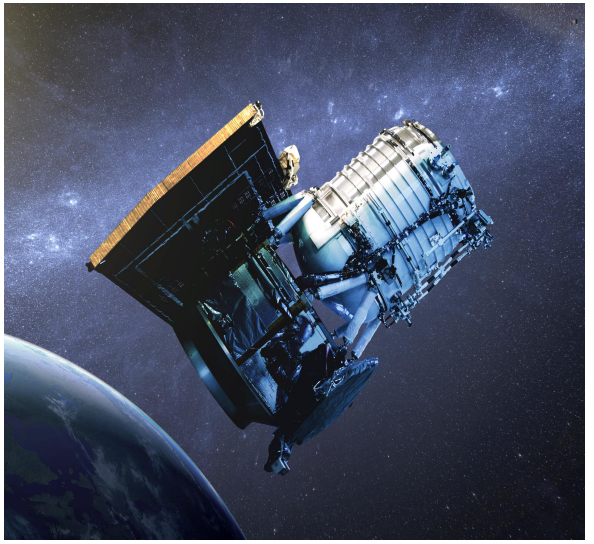

- NASA mission
- Wide-field Infrared Survey Explorer.
- 2009- Feb. 2011, hybernation, Sep. 2013-NEOWISE (Near Earth Object)
- 2021 extension of NEOWISE, decommissioned in 2024
- 40cm telescope, monitored all sky
- Sun-synchronous polar orbit = 520km above the terminator, solar panels always pointed at the Sun, telescope always looked out away from Earth and at right angle from the Sun
- 4 filters, w1-w4, 3.4, 4.6, 12, 22 micron, 8s exposures every 11s, cooled below 15K by solid hydrogen
- Asteroids, NEOs, brown dwarfs

Kepler mission

- NASA mission
- Mission launched in 2009, retired in 2018
- Schmidt telescope design, 0.95m aperture (1.4m mirror)
- One field of view of about 105deg^2, 12 deg diameter
- Cygnus-Lyra, 170000stars
- Only stars brighter than 14. mag., for 3.5 year
- 430-890 nm spectral region
- short (1min) or long (30min) cadence
- Was looking for transits and variability in reflected light from planets with the total noise <=2e-5 for 12mag star
- In reflected light giant planets with periods up to 7 days are Detectable
- K2 mission (different fields) 2014-2018

GAIA mission

- GAIA (ESA)
- Launched 2013, retired 2025
- 2 mirrors (1.45x0.5m)
- Astrometry (50x better than Hipparcos): position, parallax, proper motion
- 20 micro-arc-sec precision in position (15mag star) = 20%error in distance at the center of the Galaxy
- 3D map of our galaxy, thousands of giant planets at a few AU using astrometry
- 2 billion (10^9) objects, each star about 70x during 5 yr, up to mag 20
- L2 (Sun-Earth) orbit
- Photometry, three passbands: G=300-1100nm, G_bp=330-680 nm, G_rp=640-1050nm (from low resolution spectra, 2 prisms)
- High resolution spectroscopy 847-874nm, radial velocities 1-30 km/s precision (up to mag 17)
- GAIA DR1-2016, DR2-2018, DR3-2022, DR4-dec.2026?,DR5-?

TESS

•TESS (transiting exoplanet survey satelite), NASA+MIT, search for nearest transiting rocky planets. Launched April 2018, 2yr primary mission. First spaceborn all-sky survey (85%of sky), focus on bright stars V<10mag, 200 thousand MS dwarf stars (cooler than Kepler).

• 4 cameras, each 10cm lens in diameter, with 24x24 deg^2 field and 4 CCDs, 1pixel=21arcsec, 600-1000nm passband.

•Will tile the sky with 26 sectors (24x96 deg2), 27 days at each sector, 2min cadence, full frame images 30min cadence

•high Earth elliptical orbit, orbital period=13.7d in 2:1 resonance with the Moon

•Since July 2020 extended mission with slightly different cadence and targets near the ecliptic

•As of Nov 15, 2023 more than 6977 exoplanet candidates, suitable for follow up and JWST…, 402 confirmed

CHEOPS

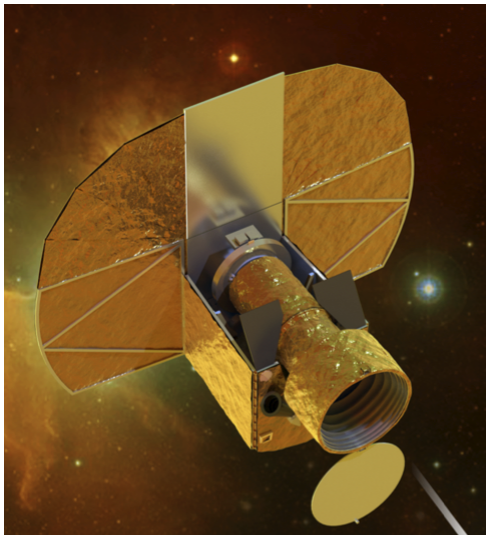

- CHEOPS (CHaracterizing ExOPlanet Satelite), high cadence (1 min) photometry, V mag<12.5, ESA S1 class mission, launched Dec 18, 2019.
- Small Ritchey-Chretien telescope, 32cm mirror, 250kg.
- 3.5 yr, 500 targets
- Single 1kx1k CCD in visible (450-950nm).
- Orbit: Sun-synchronous (precession=1yr), orbit follows day-night terminator, 650-800km altitude.
- Will perform ultra-high-precission photometry of bright stars (defocused images) already known to host planets (super-Earths and Neptunes which have masses determined) resulting in planet radius precision of about 10%.
- 20% of time devoted to the whole community.

JWST

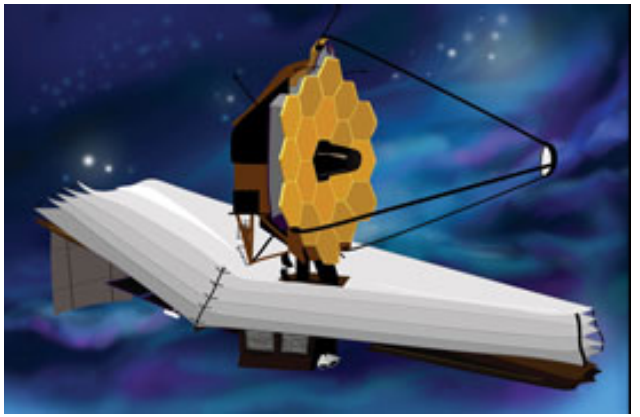

JWST (The James Webb space telescope, NASA+ESA+Canadian space agency):Infrared optimized telescope, segmented mirror, 6.5m diameter (18 folded mirrors made from light beryllium coated by gold), 6.2 ton, sun-shield. Orbit near the L2 point to shield Sun, Earth+Moon simultaneously. Four main themes: The End of the Dark Ages: First Light and Reionization, The Assembly of Galaxies, The Birth of Stars and Protoplanetary Systems, and Planetary Systems and the Origins of Life. Launched Dec 25, 2021, duration 5-10yr.

Instruments:

•The Mid-Infrared Instrument (MIRI) is an imager and spectrograph cooled to 7K. Imaging: 9 broad-band filters 5.6-25.5mic. Low resolution spectroscopy 5-12 mic, medium resolution spectroscopy 4.9-28.8mic.

•The Near Infrared Camera (NIRCam) is an imager with a large field of view and high angular resolution. Has two identical modules pointing to adjacent fields. Each module uses a dichroic to observe simultaneously in short wave. channel (0.6-2.3mic) and long wave. channel (2.4-5mic) and many filters. It also offers a wide field grism spectroscopy and coronagraphic imaging mode.

JWST

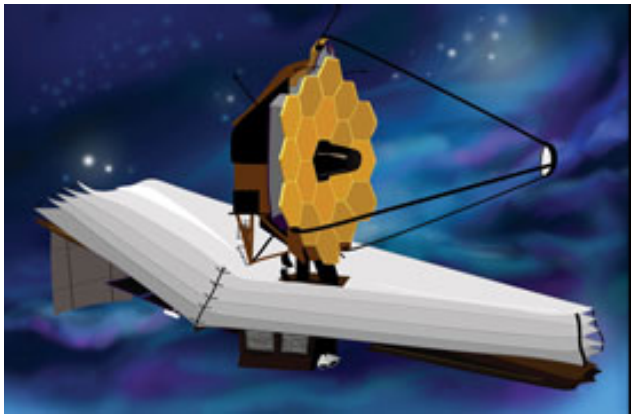

Instruments:

•Near Infrared Spectrograph (NIRSpec), 0.6-5.3 micron. Microshutter array with 4x62000 (100x200 micron) elements, 3.4x3.6 arcmin^2 field of view, will enable to observe spectra of 100 objects simultaneously. Gratings will provide resolution of 500-3600 while a prism will deliver R=30-300. Also has single object slit spectroscopy.

•The JWST Near-Infrared Imager and Slitless Spectrograph (NIRISS) provides unique observational capabilities between 0.6 and 5 µm that complement those available with NIRCam and NIRSpec. Is mounted together with FGS below.

•The Fine Guidance Sensor (FGS). It is a very broadband guide camera in order to meet the image motion requirements of the JWST. This sensor is used for both "guide star" acquisition and fine pointing.

Future: PLATO

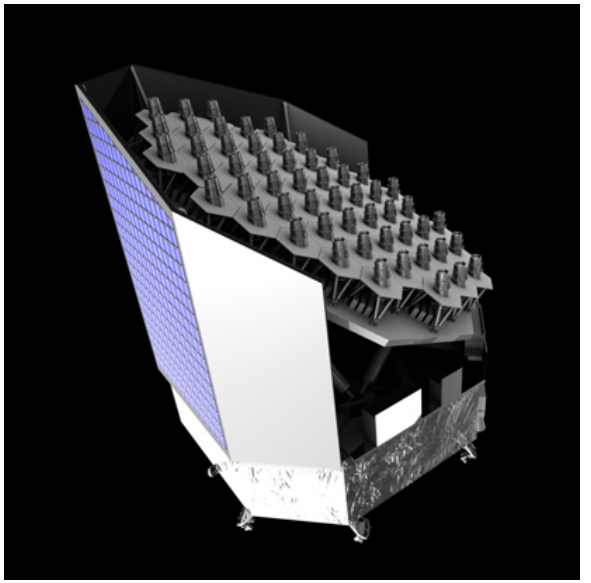

- PLATO (PLAnetary Transits and Oscillations of stars)
- ESA M3 mission, search for Earth-like planets in habitable zones around bright stars (V=4-11 mag but can reach 16 mag), launch 2026.
- CCD optical photometry
- 24 cameras (4 groups of 6), each camera is a small 12 cm telescope, 25s cadence for m_v>8mag + 2 fast cameras with 2.5s cadence for bright stars with m_v=4-8mag, 1pix=15”
- wide field of view (2232 deg2), 50% of the sky, 1 milion stars, 2x2yr
- Orbit: libration around L2
- Wavelengths: optical
- detection->radii +
- ground based radial velocity follow-up -> planet masses +
- Asteroseismology for the determination of stellar masses, radii, and ages +
- identification of bright targets for atmospheric spectroscopy

Future: NGRST

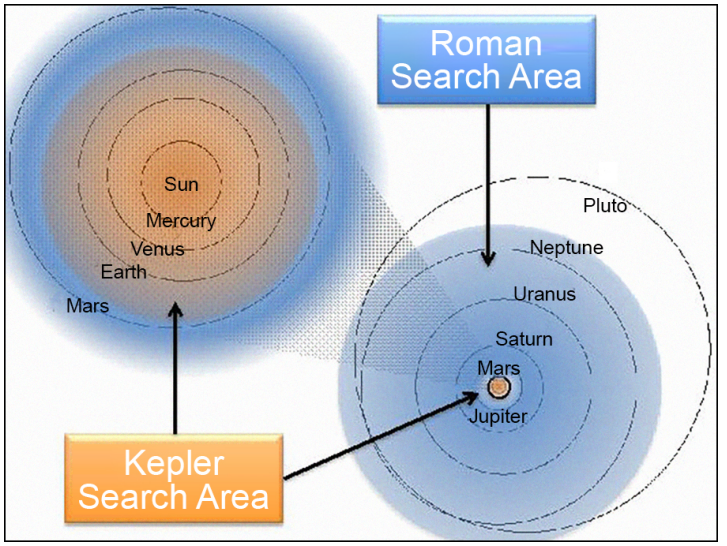

Nancy Grace Roman Space telescope
(formerly known as WFIRST=Wide Field InfraRed Survey Telescope)
NASA, top-ranked large astrophysics mission, cosmology & exoplanets,
designed to unravel the secrets of dark energy and dark matter,
search for and image exoplanets, and explore many topics in infrared
astrophysics.

2.4m telescope, similar to Hubble but FoW is 100x larger

A/ Wide field instrument: Imaging, 0.28deg^2, 0.1 arcsec/pix
0.48-2.3mic range, 1 wide+6 narrow filters
Slitless spectroscopy
Microlensing search for exoplanets, 100mil stars

B/ Coronograph and direct imaging and spectroscopy of exoplanets
(>0.15arcsec from the star) & debris disks, optical range 0.5-0.8mic

Will orbit around the L2/Sun/Earth point.
Launch: affected by Covid but not later than 2027

Future: ARIEL

- ARIEL (Atmospheric Remote-sensing Infrared Exoplanet Large-survey)
- ESA, medium-class science mission, launch in 2029
- Off-axis Cassegrain 1.1x0.7m class telescope

- Targets: 1000 known exoplanets, focus on warm and hot exoplanets

- Goal: investigate the atmospheres using transit method, their chemical composition, thermal structure, how planetary systems form and evolve

- Imaging visible+NIR
- Spectrometer IR

Future missions: interior

•JUNO (NASA):

How much water is in Jupiter's atmosphere, which helps determine which planet formation theory is correct (or if new theories are needed). Look deep into Jupiter's atmosphere to measure composition, temperature, cloud motions and other properties. Map Jupiter's magnetic and gravity fields, revealing the planet's deep structure. Explore and study Jupiter's magnetosphere near the planet's poles, especially the auroras – Jupiter's northern and southern lights – providing new insights about how the planet's enormous magnetic force field affects its atmosphere. Launch - August 5, 2011, arrived at Jupiter - July 2016, extended to 2025 to study moons of Jupiter.

• Bepicolombo (ESA+JAXA(Japan)):

European first mission to Mercury. It will study the composition and history of Mercury, but also on the history and formation of the inner planets in general, including Earth. The science mission will consist of two separate spacecrafts. Mercury Planetary Orbiter will study the surface and internal composition of the planet, and the Mercury Magnetospheric Orbiter will study Mercury's magnetosphere. Launched in 2018 and will arrive at Mercury in 2025.

•JUICE - JUpiter ICy moons Explorer:

large-class mission, ESA. Launched in April 2023 and arrival at Jupiter in 2031, detailed investigations of Ganymede and its potential to support life, investigations of Europa and Callisto (all three moons probably have subsurface liquid water oceans, chemistry + organic molecules.

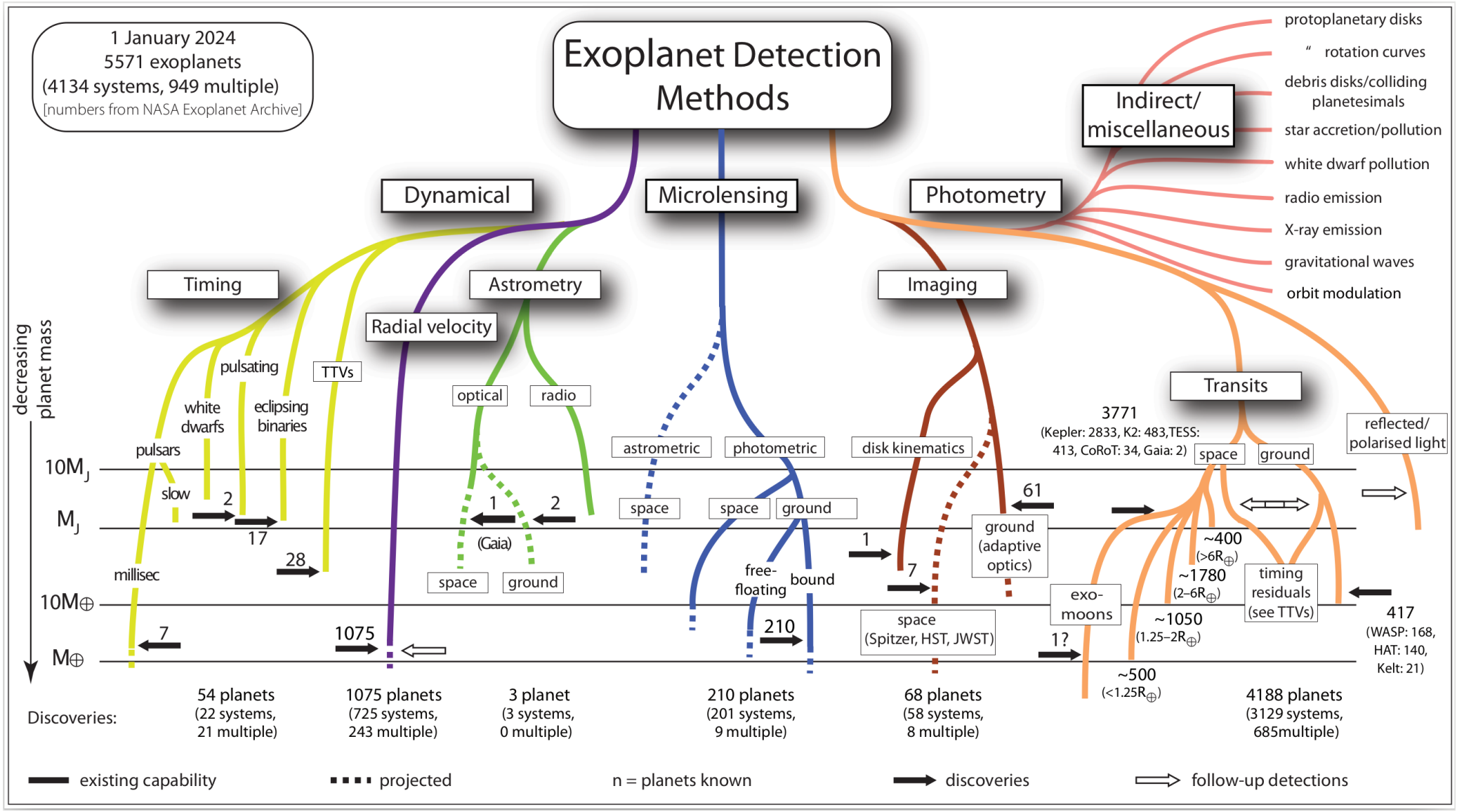

Radial velocity variation

Planet is not visible. We observe the spectral lines and movement of the star.
Radial Velocity (RV) is positive when object is departing i.e. redshifting.
Amplitude of the RV curve depends on the planet's orbital period, mass, and inclination => degeneracy between m_p & i.

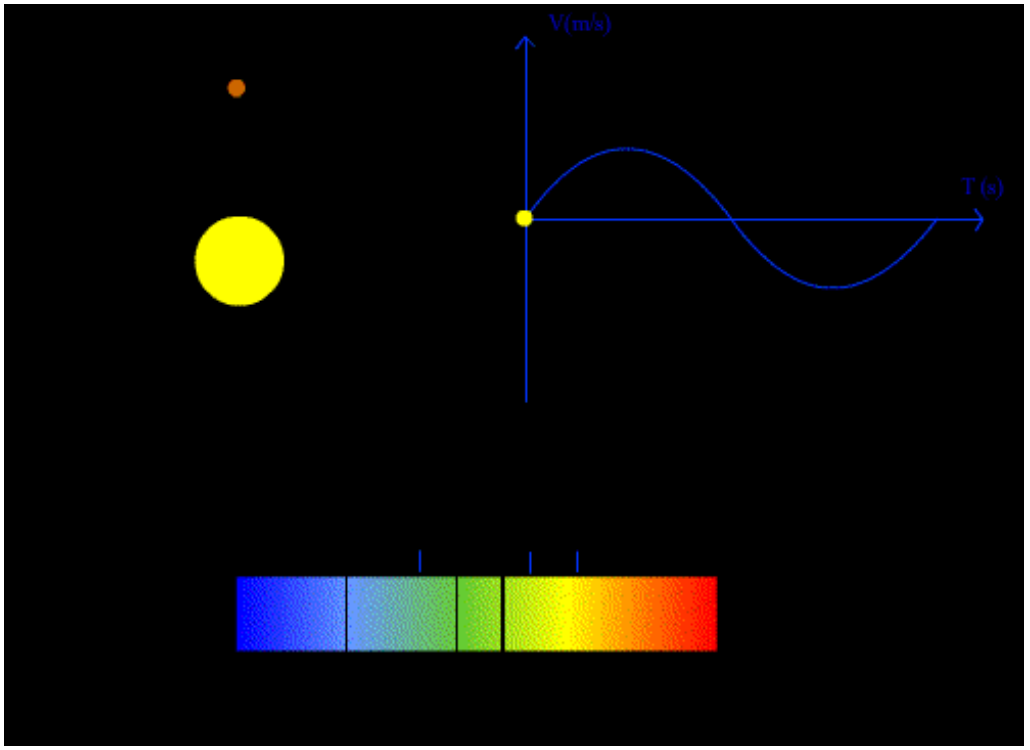

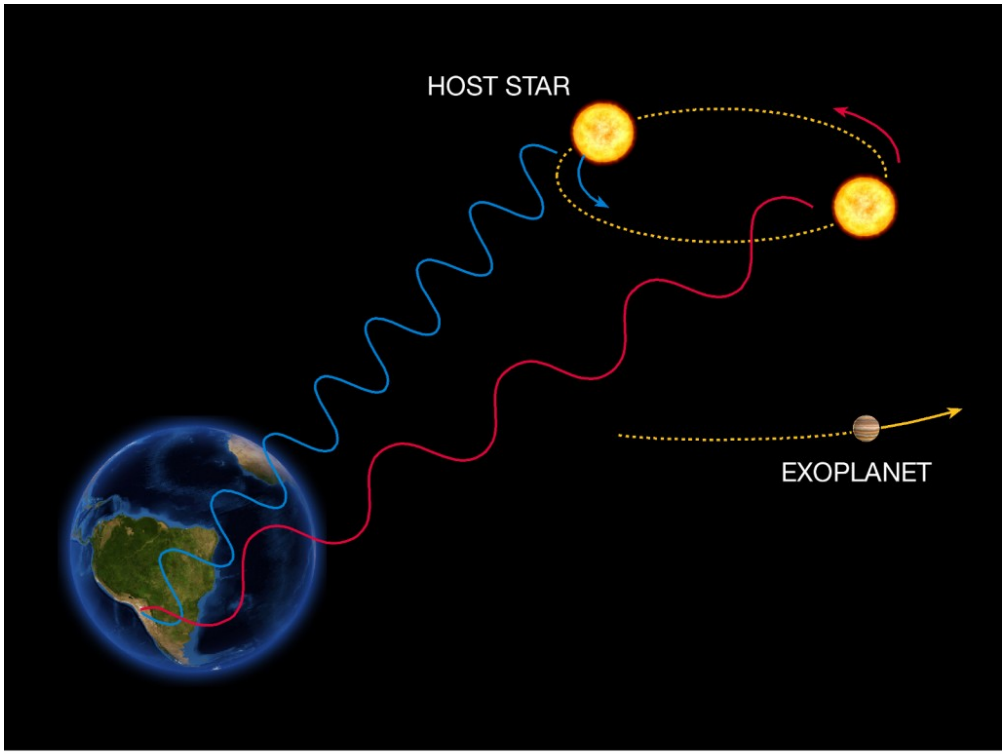

The Radial Velocity Method

ESO Press Photo 22e/07 (25 April 2007)

Radial velocity variation

Orbital elements of the moving star (not all can be determined):

i – inclination of the orbit from the plane of sky
Ω - ascending node of the line of nodes (longitude of the ascending node, object recedes) measured in the plane of sky from N
ω – argument of periastron (π) measured from Ω in the direction of motion
a - semi-major axis
e – eccentricity
P – orbital period
T – epoch of periastron passage
+
υ – true anomaly (measured from π in the direction of motion)
γ - center of mass velocity

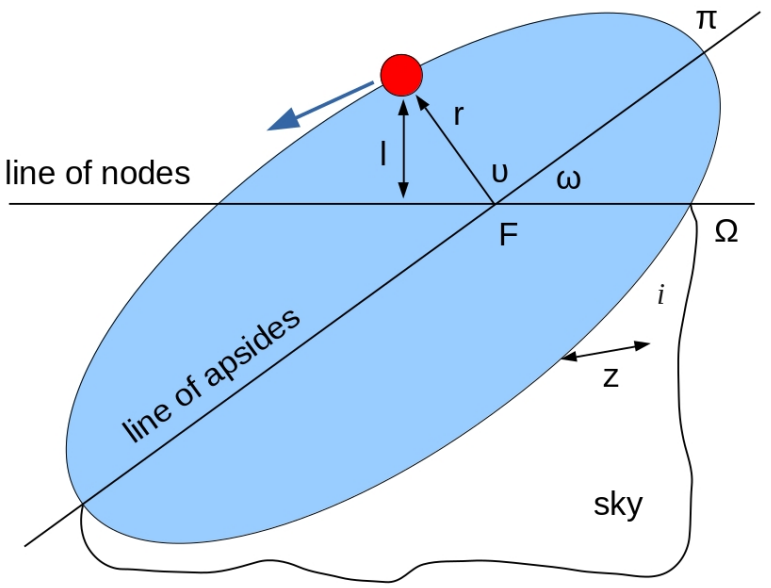

$$l(t) = r(t)\sin(\upsilon + \omega)$$

Distance from the line of nodes

$$z(t) = r(t)\sin(\upsilon + \omega)\sin i$$

Radial distance

$$v_r = \gamma + \dot{z}(t) = \gamma + \sin i \sin(\upsilon + \omega)\dot{r} + r \sin i \cos(\upsilon + \omega)\dot{\upsilon}$$

Radial velocity

Radial velocity variation

$$v_r = \gamma + \dot{z}(t) = \gamma + \sin i \sin(\upsilon + \omega)\dot{r} + r \sin i \cos(\upsilon + \omega)\dot{\upsilon}$$

$$v_r = \gamma + \frac{2\pi\, a \sin i}{P\sqrt{(1-e^2)}}\left[e\cos\omega + \cos(\upsilon+\omega)\right]$$

$$r = \frac{a(1-e^2)}{1+e\cos\upsilon}$$

$$\dot{r} = \frac{a(1-e^2)e\sin\upsilon}{(1+e\cos\upsilon)^2}\dot{\upsilon}$$

$$r^2\dot{\upsilon} = 2\pi\, a^2\sqrt{1-e^2}/P$$

second Kepler's law

$$v_r = \gamma + K\left[e\cos\omega + \cos(\upsilon+\omega)\right] \qquad K = \frac{2\pi\, a \sin i}{P\sqrt{(1-e^2)}}$$

Extrema:

$$v_{max} = \gamma + K\left[e\cos\omega + 1\right] \qquad for \quad \upsilon = -\omega$$

$$v_{min} = \gamma + K\left[e\cos\omega - 1\right] \qquad for \quad \upsilon = \pi - \omega$$

$$v_{max} - v_{min} = 2K$$

=> K -is semi-amplitude of the radial velocity curve regardless of its shape. Maxima RV are at nodes!

Radial velocity variation

This is the radial velocity (rv) curve as a function of true anomaly. We need to connect the true anomaly with time to get rv curve as a function of time:
t → M → E → υ

$$v_r = \gamma + K\left[e\cos\omega + \cos(\upsilon + \omega)\right]$$

$$K = \frac{2\pi a \sin i}{P\sqrt{(1-e^2)}}$$

t – time

T - time at periastron

M – mean anomaly

E - eccentric anomaly

υ – true anomaly

$$\frac{2\pi}{P}(t-T) = M = E - e\sin E$$

Kepler's equation

$$\tan\frac{\upsilon}{2} = \sqrt{\frac{1+e}{1-e}}\tan\frac{E}{2}$$

Observations: (rv,t) can be fit by the least square or other minimization method.
Ultimately one can determine these orbital elements:
γ, K, e, ω, P, T. Or alternatively: γ, asini, e, ω, P, T.
One cannot determine the inclination and thus the semi-major axis. Apart from that one can determine the mass function.

Radial velocity variation

How to get planet mass from rv curve?
Star: m1,a1, planet: m2, a2

$$a_2/a_1 = m_1/m_2 \qquad a_1 + a_2 = a_1(1 + a_2/a_1) = a_1(m_2/m_2 + m_1/m_2)$$

$$(a_1 + a_2)^3 = \frac{a_1^3}{m_2^3}(m_2 + m_1)^3 \qquad (a_1 + a_2)^3 = \frac{G}{4\pi^2}(m_1 + m_2)P^2$$

$$K = \frac{2\pi\, a \sin i}{P\sqrt{(1-e^2)}}$$

$$\frac{a_1^3}{m_2^3}(m_2 + m_1)^3 = \frac{G}{4\pi^2}(m_1 + m_2)P^2$$

$$a_1 \sin i = \sqrt{(1-e^2)}\,\frac{K_1 P}{2\pi}$$

$$a_1^3 \sin^3 i = \frac{G}{4\pi^2}P^2 \frac{m_2^3 \sin^3 i}{(m_1+m_2)^2} \equiv \frac{G}{4\pi^2}P^2 f(m_2)$$

$$f(m_2) \equiv \frac{m_2^3 \sin^3 i}{(m_1+m_2)^2} \qquad f(m_2) = \frac{4\pi^2 a_1^3 \sin^3 i}{G P^2} = \frac{P(1-e^2)^{3/2} K_1^3}{2\pi G}$$

Mass function

From only one radial velocity curve of m1 one can get the mass function of m2 only.

Radial velocity variation

Similar to the SB1 spectroscopic binary and from one radial velocity curve you get: P, T, e , ω, K, γ and then:

$$f(m)=\frac{m^3 \sin^3 i}{(M+m)^2}=1.0385\,10^{-7}(1-e^2)^{3/2}K^3 P \Rightarrow m\sin(i)\approx f(m)^{1/3}M^{2/3}$$

$$a\,sini=13751\sqrt{(1-e^2)}\,K\,P$$

K -semi-amplitude in km/s, P -period in days, f(m) -mass function in Msol, a -semi-major axis in km, e -eccentricity, ω -longitude of periastron, γ -center of mass velocity, msini -minimum mass of the planet

- Advantages: can get 5 orbital elements + msini, a sini, precision 1m/s, hot Jupiters can be detected with sub-1m class telescopes

- Disadvantages: strong bias to close in planets and high inclination, unknown inclination, precision limit of about 1m/s set by the stellar activity and oscillations (ESO-HARPS instrument), stars must have many lines, lines must be sharp, object must be non variable, only can be applied to F and later sp. type.

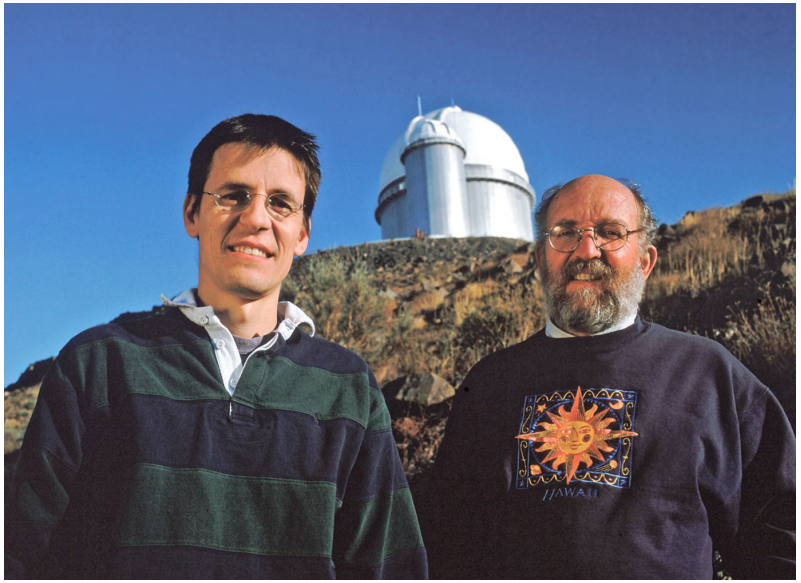

Nobel prize 2019

The Nobel Prize in Physics 2019 was awarded "for contributions to our understanding of the evolution of the universe and Earth's place in the cosmos" with one half jointly to Michel Mayor and Didier Queloz "for the discovery of an exoplanet orbiting a solar-type star."

(visited Slovakia in 2011, Z.G.)

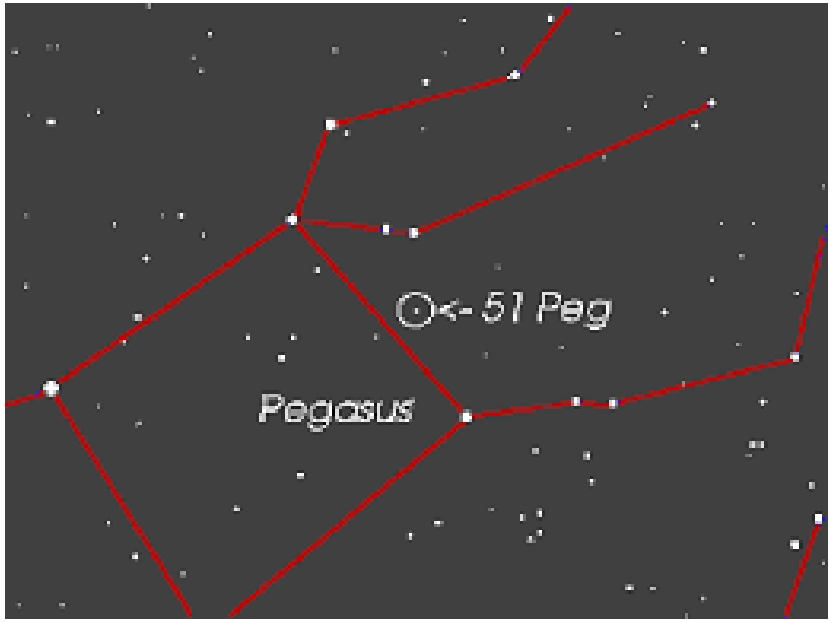

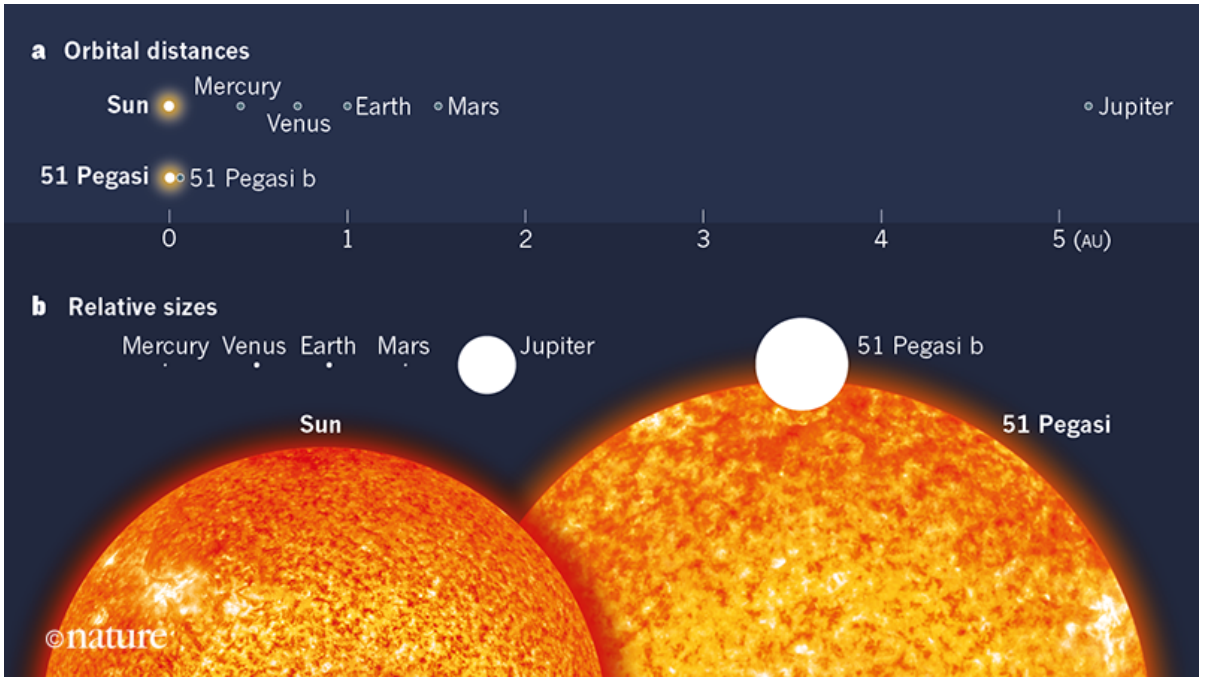

51 Peg b (Dimidium='half')

Instrument used by Mayor & Queloz:

-fiber fed echelle spectrograph ELODIE (R=42000, AA 3910-6810)

-1.93m telescope, Haute-Provence Obs., France

-radial velocity was measured from thousands of spectral lines using cross-correlation, precision 13m/s

-excluded spots & pulsations

Result: P=4.23 d, e=0, msini=0.47+-0.02M_J

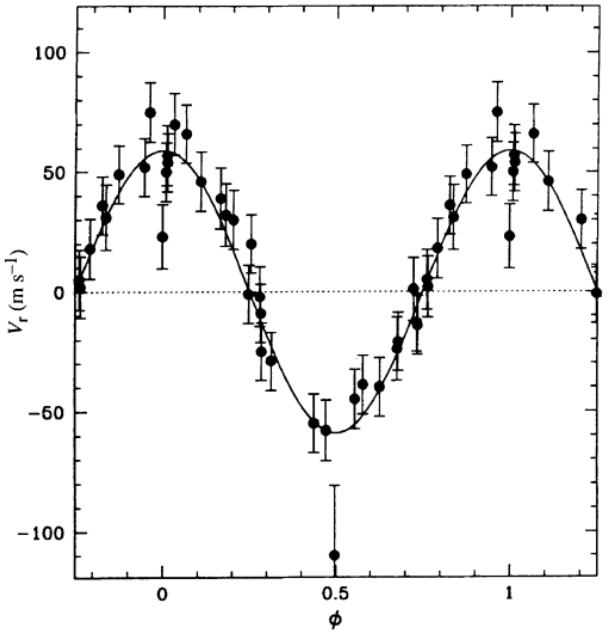

51Peg, Mayor & Queloz 1995

This discovery raised new questions, launched an intense hunt for exoplanets, and a new field of research emerged.

51 Peg b

Why is the mass of 51Pegb 2dex lower than that of lowest mass companions?

Why there were no objects -3<logM<-1?

Solar system does not have a Hot Jupiter.

Do most stars have Hot Jupiters?

How come Hot Jupiters exist?

Is our solar system unique?

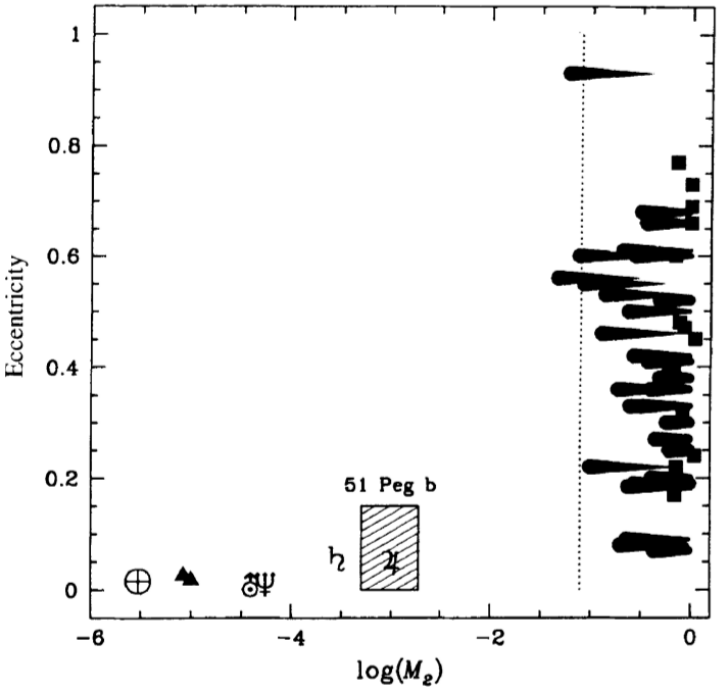

51Peg, Mayor & Queloz 1995

Transit of the planet

Transit (smaller object in the front)=primary eclipse (cooler object in the front)
Occultation (smaller object in the back)=secondary eclipse (cooler object in the back)
smaller=smaller angular dimension as seen from Earth

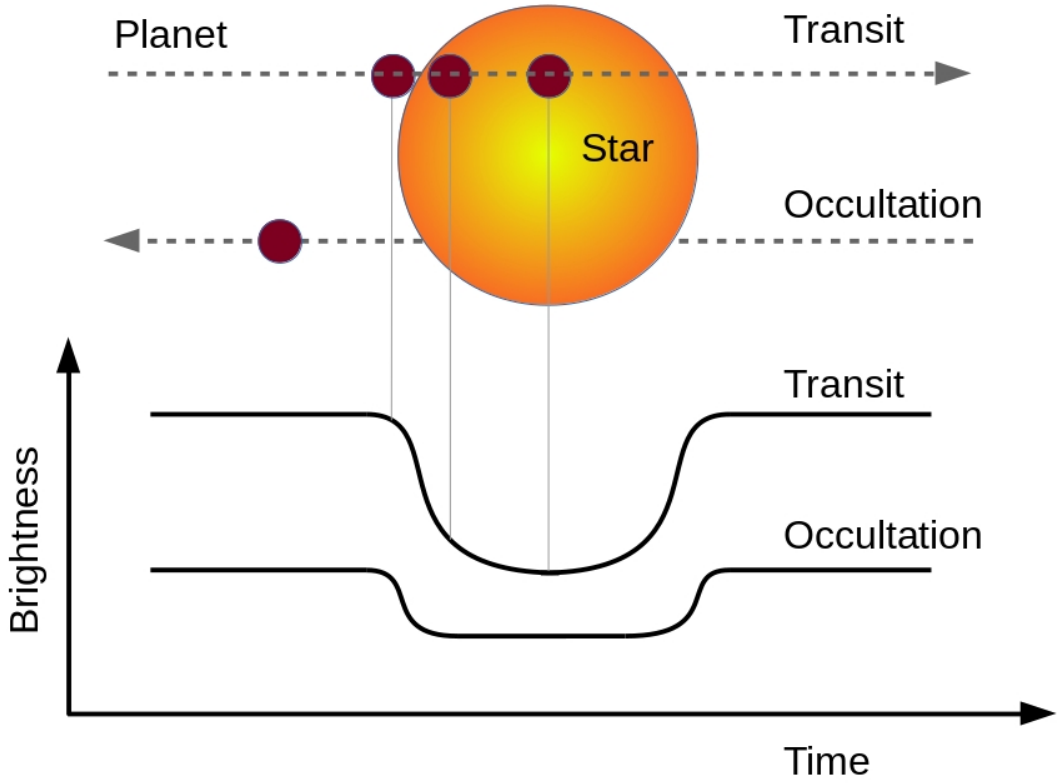

Schematic light curve assuming a total eclipse of a smaller and cooler object (R2,T2,L2) by a bigger and hotter object (R1,T1,L1), circular orbits, and no limb darkening:

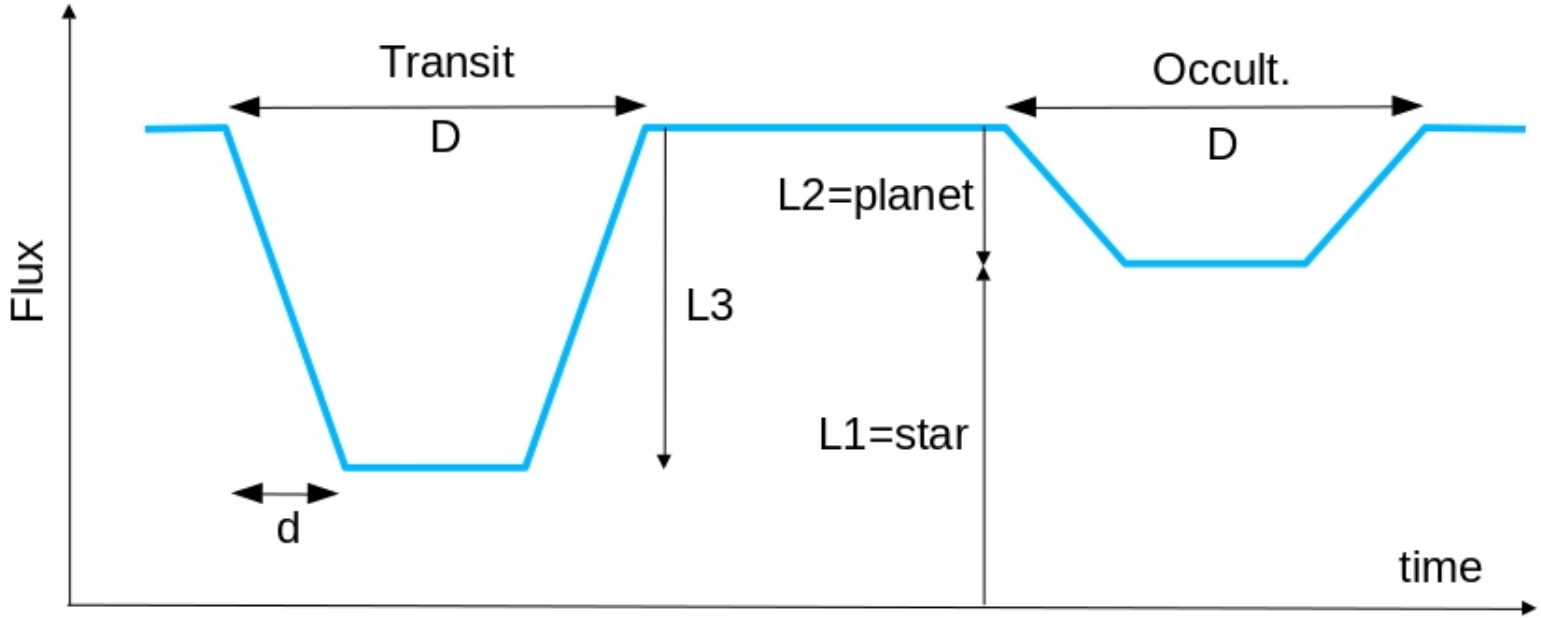

Transit, occultations depths:

$$\pi R_1^2 \sigma T_1^4 \sim L1 \qquad \pi R_2^2 \sigma T_1^4 \sim L3 \qquad \pi R_2^2 \sigma T_2^4 \sim L2$$

$$\frac{R_2^2}{R_1^2} = \frac{L3}{L1} \qquad \frac{T_2^4}{T_1^4} = \frac{L2}{L3}$$

Transit durations: $v = 2\pi a/P$

$$2R_2 \sim v\,d, \quad 2(R_1+R_2) \sim v\,D$$

$$d \sim R_2/a, \quad D \sim (R_1+R_2)/a$$

Rayleigh-Jeans tail:

$$\frac{T_2}{T_1} = \frac{L2}{L3}$$

$$\frac{R_1}{a}, \frac{R_2}{a}$$

Transit of the planet

•Analysis:
-synthetic light-curves are computed and fit to the data,
-effect of limb darkening must be included,
-requires the stellar radius (Teff+distance, interferometry, oscillations) or
-stellar mass (assuming 3.Kepler's law+period → a)
-one can get both radii, inclination and the semi-major axis

•Advantages:
-simple photometry from the ground and space, small telescopes,
-provides planetary radii and inclination,
-can be combined with radial velocities to get planetary masses,
-offers transit radius spectrum and occultation spectroscopy,
-enables to search for transit timing variations (TTV), transit duration variations (TDV).

•Disadvantages:
-strong bias for the large planets and close in orbits (edge-on orbits),
-planets smaller than Neptune require small but space-based telescopes.

Transit probability

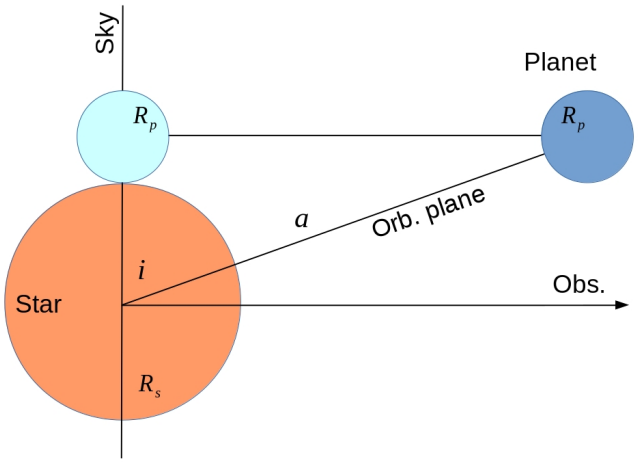

Transit requires: $a\cos i < R_{star} + R_{planet}$

$$\cos i_{min} = \frac{R_{star} + R_{planet}}{a} \approx \frac{R_{star}}{a}$$

Solid angle swept out by the orbital axes 0<i<imin is a non-transiting cone:

$$\omega_{nt} = 2\pi\left(1 - \cos i_{min}\right)$$

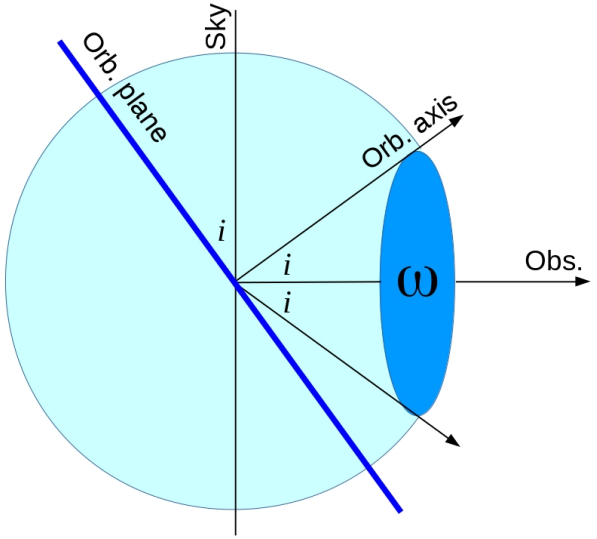

Non-transit probability, divide by half the space angle:

$$P_n = \frac{\omega_{nt}}{2\pi} = \frac{2\pi\left(1 - \cos i_{min}\right)}{2\pi} = 1 - \cos i_{min}$$

Transit probability:

$$1 - P_n = \cos i_{min} \approx \frac{R_{star}}{a}$$

Timing

We have a source producing pulses with period P_0. The source is at the distance z_0. We measure arrival time of pulses O(observed) and compare with the expected or calculated time C(calculated) and calculate the residuals O-C. If the distance of the source does not change, O-C(t) is a strait line. Let's assume a planet and that the source moves on an elliptical Keplerian orbit around the center of mass. Its radial distance changes:

$$z(t)=r(t)\sin(\upsilon+\omega)\sin i \qquad r=\frac{a(1-e^2)}{1+e\cos\upsilon}$$

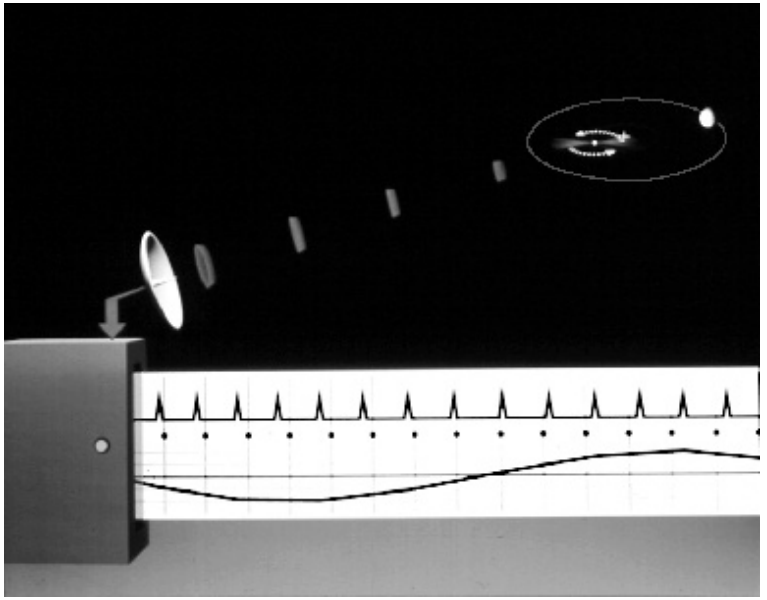

Pulses will be delayed due to light travel time:

$$(O-C)=(z-z_0)/c$$

$$(O-C)=\frac{a\sin i(1-e^2)}{c}\frac{\sin(\upsilon+\omega)}{1+e\cos\upsilon}$$

It is similar to radial velocity method where

$$a_1^3\sin^3 i=\frac{G}{4\pi^2}P^2\frac{m_2^3\sin^3 i}{(m_1+m_2)^2}$$

For circular orbit and m2<<m1:

$$(O-C)=\frac{1}{c}a\sin i\sin\left(2\pi\frac{t-T}{P}\right)$$

$$\frac{a\sin i}{c}=1.5[ms]\left(\frac{m_2}{m_{Earth}}\right)\left(\frac{m_1}{m_{Sun}}\right)^{-2/3}\left(\frac{P}{yr}\right)^{2/3}\sin i$$

In pulsars we can measure the O-C amplitude with precision of microseconds which enables to discover planets with the mass of 0.01Earth i.e. that of Moon.

Timing

If we use the derivative of O-C (or Doppler effect applied to pulse frequency) we get the radial velocity curve. It means that the problem is equivalent to the radial velocity method and we can derive the same orbital elements: gamma, K, e, omega, P, T. Alternatively: asini, msini.

1st exopl. PSRB1257+12 (Wolszczan & Frail 1992): 3:2 resonance, perturb. -> true masses, coplanar, disk origin...

	m(me)	P(d)	e	i
b	4.3	66.5	0.0182	53
c	3.9	98.2	0.0264	47
d	0.015/sini	25.3	0	

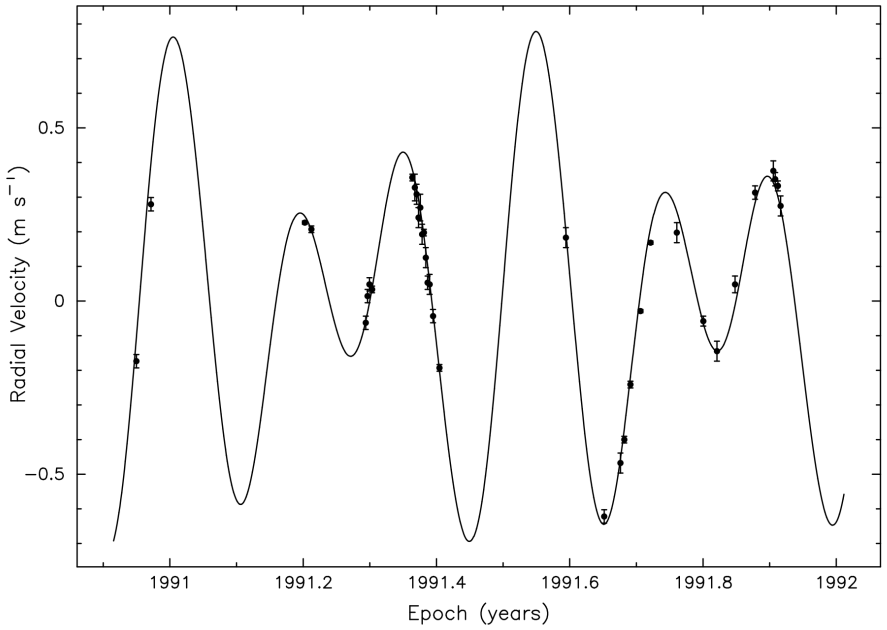

$$\frac{d(O-C)}{dt} = \dot{z}/c$$

$$P = \frac{1}{\nu} \qquad \delta P = -\frac{\delta \nu}{(\nu)^2} = -\frac{\delta \nu}{\nu} P$$

$$\frac{\delta(O-C)}{\delta t} = \frac{\delta P}{P} = -\frac{\delta \nu}{\nu} = \frac{v_r}{c}$$

$$v_r = \gamma + K\left[e\cos\omega + \cos\left(\upsilon + \omega\right)\right]$$

$$K = \frac{2\pi a \sin i}{P\sqrt{\left(1-e^2\right)}} \qquad f(m_2) \equiv \frac{m_2^3 \sin^3 i}{(m_1+m_2)^2}$$

Changes in the rotational period of PSRB1257+12 converted to radial velocities (Wolszczan 2008). Notice the extraordinary precision of the method (cm/s) in comparison e.g. with contemporary radial velocity method.
Starting from 1991, after 3 orbits of the inner body the two planets meet again after 66x3=200d=0.55yr (in 1991.55).

Timing

- Light time effect (similar to Roemer experiment 1676, eclipses Io-Jupiter)
- PSRB1620-26 b, milisecond pulsar+WD=191d, Planet Porb=100yr (Backer et al. 1993) first circumbinary planet
- V391Peg b, pulsating sdB star (Silvotti et al. 2007)
- HW Vir bc, eclipse timing, eclipsing binary sdB+M (Lee et al. 2009), -not confirmed!
- DP Leo b, eclipse timing, eclipsing binary AM Her

- Advantage: can detect planets as small as 0.01 Earth mass
- Disadvantage: pulsars are rare, cannot expect life

- Eclipse timing variability (ETV) is similar
- Transit timing variability (TTV) is different (usually involves dynamical interaction between planets)

Timing, O-C diagram

O-C (observed-calculated). Expected time of n-th eclipse:

$$C_n = T_0 + nP_0$$

Observed time of n-th eclipse with a period shift:

$$P = P_0 + \delta P \qquad O_n = T_0 + n(P_0 + \delta P)$$

Result is a linear curve in O-C diagram:

$$O_n - C_n = n\,\delta P = \frac{t - T_0}{P}\,\delta P$$

Assuming linear period change:

$$P = P_0 + b(t - T_0)$$

$$O_n = T_0 + \int_0^n P\,di = T_0 + nP_0 + \int_0^n b\,(t - T_0)\,di$$

$$P \approx \frac{\delta t}{\delta i} \qquad di = \frac{dt}{P} \qquad b = \frac{dP}{dt}$$

$$O_n = T_0 + nP_0 + b\int_{T_0}^{t} (t - T_0)/P\,dt$$

$$O_n = T_0 + nP_0 + \frac{b}{2P}(t - T_0)^2$$

$$O_n - C_n = \frac{b}{2P}(t - T_0)^2$$

Period change is very small on human timescales so P is almost constant → Parabola in O-C diagram:

$$Model\ A: \quad P_0 = 1\,d$$

$$Model\ B: \delta p = +0.01\,d\,(HJD < 500\,d)$$

$$\delta p = -0.02\,d\,(HJD > 500\,d)$$

$$Model\ C: \quad b = \frac{dP}{dt} = 2.3\,x\,10^{-10} \qquad \frac{P}{\dot{P}} = 10^7\,yr$$

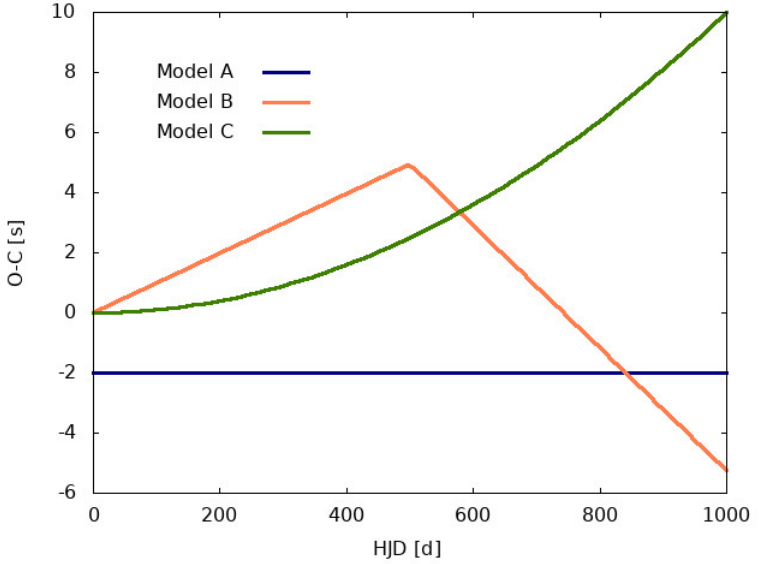

Gravitational microlensing

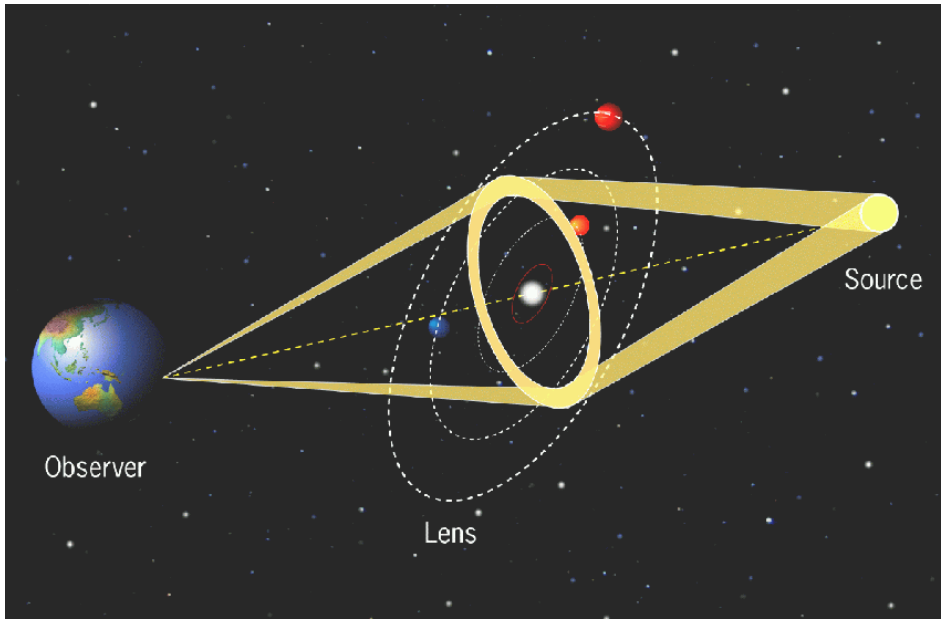

Lens=magnification, objects are moving → lightcurve, e.g. OGLE-2005-BLG-390 (Mp=5.5MEarth, a=2.6au, Beaulieu et al. 2006):

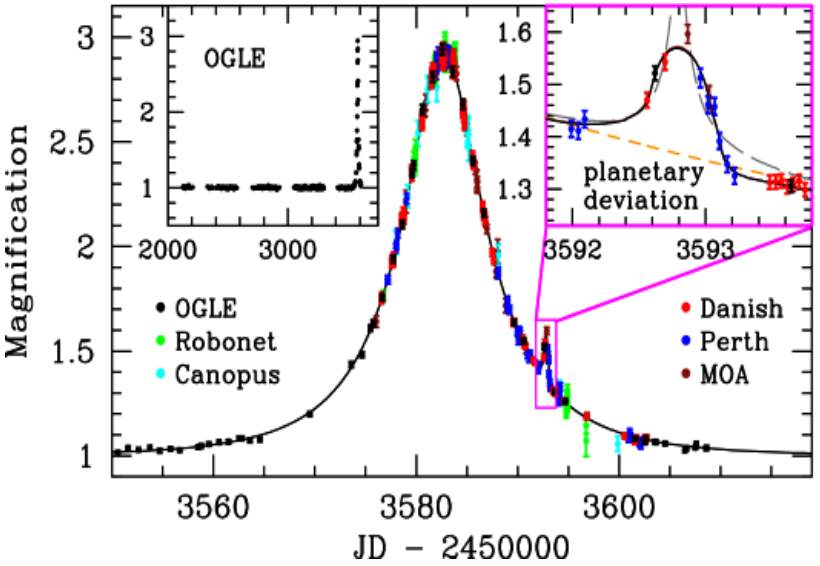

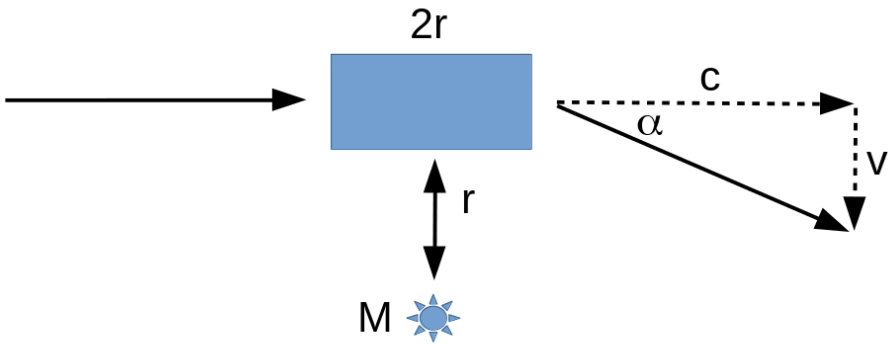

Heuristic Newtonian light deflection by a mass -M with the impact parameter -r:

$$v = a\,t \qquad a \approx \frac{GM}{r^2} \qquad t = \frac{2r}{c}$$

$$v = \frac{2GM}{rc} \qquad \alpha = \frac{v}{c} = 2\frac{GM}{c^2 r}$$

Gravitational microlensing

General theory of relativity:
light passing by a mass -M
with the impact parameter -r
is deflected by an angle α.
R_s is Schwarzschild radius.

$$\alpha = 4\frac{GM}{c^2 r} = 2\frac{R_S}{r}, \qquad R_S \equiv 2\frac{GM}{c^2}$$

Θ_S is true angle to the source,
Θ is apparent angle to the source,
Θ_E is Einstein ring

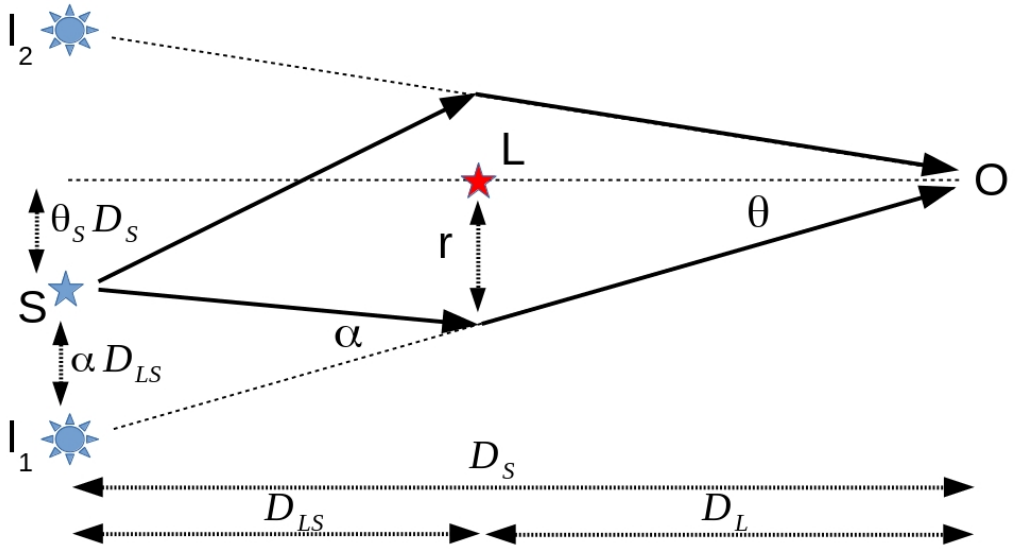

S=Source, L=Lens, O=Observer, I1/I2=Images, DL/DS=Distance to the Lens/Source

Let's calculate the location of images

$$\theta D_S - \theta_S D_S - \alpha D_{LS} = 0$$

$$\theta_S = \theta - \alpha\frac{D_{LS}}{D_S}$$ Lens equation

$$\theta - \theta_S - \frac{2R_S}{r}\frac{D_{LS}}{D_S} = 0 \qquad r = \theta D_L$$

$$\theta^2 - \theta_S\theta - 2R_S\frac{D_{LS}}{D_S D_L} = 0$$

$$\theta_E^2 \equiv 2R_S\frac{D_{LS}}{D_S D_L}$$

$$\theta^2 - \theta_S\theta - \theta_E^2 = 0$$

Gravitational microlensing

$$\theta^2 - \theta_S \theta - \theta_E^2 = 0$$

Two solutions: $$\theta_{1,2} = \frac{1}{2}\left(\theta_S \pm \sqrt{\theta_S^2 + 4\theta_E^2}\right)$$

1st special case: $\theta_S = 0 \quad \rightarrow \quad \theta_1 = -\theta_2 = \theta_E$ Einstein ring

2nd special case: $\theta_S \gg \theta_E \quad \rightarrow \quad \theta_1 = \theta_S, \quad \theta_2 = 0$

general case: $\theta_S > 0$ One image is outside the other is inside of the ring on the opposite side:

$$\theta_1 = \frac{1}{2}\left(\theta_S + \sqrt{\theta_S^2 + 4\theta_E^2}\right) > \frac{1}{2}\left(\sqrt{4\theta_E^2}\right) \quad \rightarrow \quad \theta_1 > \theta_E$$

$$-\theta_2 = \frac{1}{2}\left(\sqrt{\theta_S^2 + 4\theta_E^2} - \theta_S\right) < \frac{1}{2}\left(\theta_S + 2\theta_E - \theta_S\right) \quad \rightarrow \quad \theta_2 \in \left(-\theta_E, 0\right)$$

We made use of this relation based on Pythagorean theorem with the legs $\Theta_{S,}, 2\Theta_E$

$$\sqrt{\theta_S^2 + 4\theta_E^2} < \theta_S + 2\theta_E$$

Gravitational microlensing

$$\theta_{1,2}=\frac{1}{2}\left(\theta_S \pm \sqrt{\theta_S^2+4\,\theta_E^2}\right)$$

General theory of relativity => surface brightness is not changed by the lensing process => observable amplification of the flux is given by the ratio of the solid angles subtended by the image and its source. Picture shows mapping between elements of the source and its image on the sky:

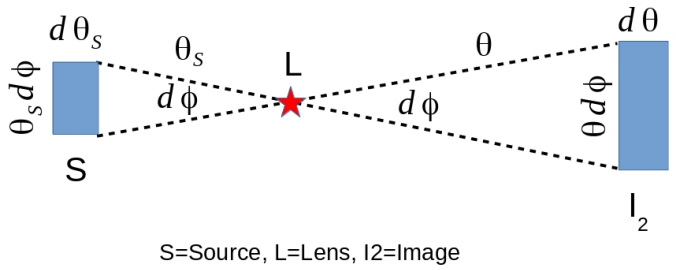

S=Source, L=Lens, I2=Image

$$u\equiv\frac{\theta_S}{\theta_E} \qquad du=\frac{d\,\theta_S}{\theta_E} \qquad u\,du=\frac{\theta_S\,d\,\theta_S}{\theta_E{}^2}$$

$$\frac{\theta_{1,2}}{\theta_E}=\frac{1}{2}\left(u\pm\sqrt{u^2+4}\right)$$

$$\frac{d\,\theta_{1,2}}{\theta_E}=\frac{1}{2}\left(1\pm\frac{u}{\sqrt{u^2+4}}\right)du$$

after...

$$\frac{\theta_{1,2}\,d\,\theta_{1,2}}{\theta_E{}^2}=\frac{1}{2}\left(u\pm\frac{u^2+2}{\sqrt{u^2+4}}\right)du$$

$$A=\frac{d\,\omega}{d\,\omega_S}=\left|\frac{\theta d\,\phi d\,\theta}{\theta_S d\,\phi d\,\theta_S}\right|=\left|\frac{\theta d\,\theta}{\theta_S\,d\,\theta_S}\right|$$

$$\left|\frac{\theta_{1,2}\,d\,\theta_{1,2}}{\theta_S\,d\,\theta_S}\right|=\frac{1}{2}\left(\frac{u^2+2}{u\sqrt{u^2+4}}\pm 1\right)$$

$$A(u)=A_1+A_2=\frac{u^2+2}{u\sqrt{u^2+4}}$$

Note if u>>1 then A2 → 0.

Gravitational microlensing

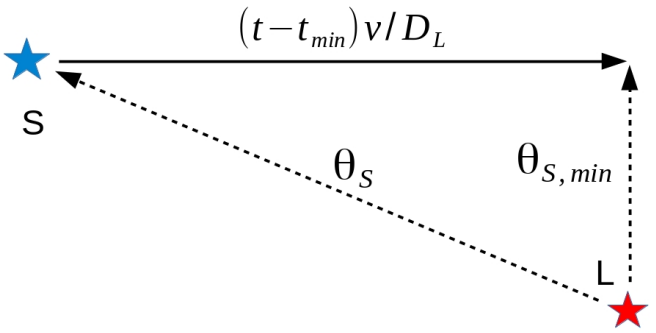

The amplification changes with time since u changes with time due to mutual transverse velocity, v, of L and S.

$$u \equiv \frac{\theta_s}{\theta_E} \qquad u_{min} \equiv \frac{\theta_{S,min}}{\theta_E}$$

$$\theta_S^2 = (t-t_{min})^2 \frac{v^2}{D_L^2} + \theta_{S,min}^2$$

$$\frac{\theta_S^2}{\theta_E^2} = (t-t_{min})^2 \frac{v^2}{D_L^2 \theta_E^2} + \frac{\theta_{S,min}^2}{\theta_E^2}$$

$$A(u(t)) = \frac{u^2+2}{u\sqrt{u^2+4}}$$

$$u(t) = \sqrt{(t-t_{min})^2 \frac{v^2}{D_L^2 \theta_E^2} + u_{min}^2}$$

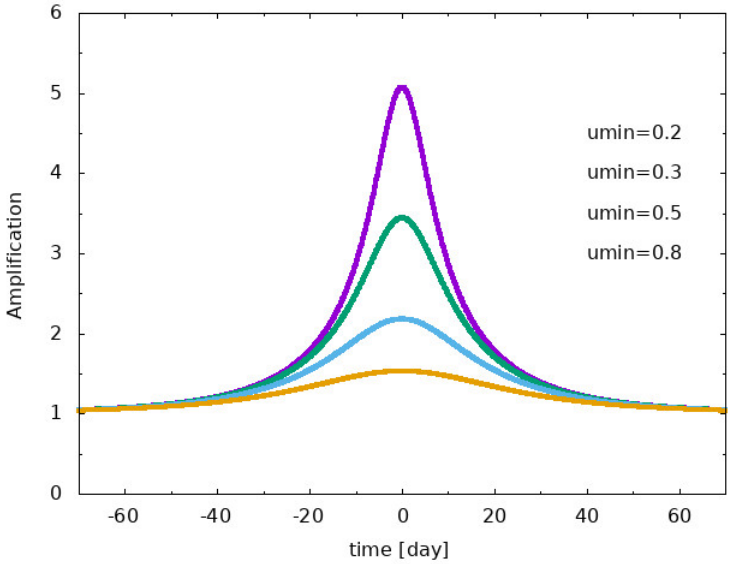

Symmetric, max at umin. Decreasing but >1.
Smaller umin=>lager A.
Amax=1/umin for strong lensing.
u=0=>A=infty, in reality A is final since source is not a point but has a final dimension
(← M=1Msol, DL=DLS=3.5kpc, v=200km/s)

Gravitational microlensing

$$\vec{\theta}_S = \vec{\theta} - \frac{D_{LS}}{D_S}\left(\vec{\alpha}_1 + \vec{\alpha}_2\right)$$

Binary lens equation in case of 2bodies, 1D->2D generalization. It describes mapping between theta_S and theta i.e. source and images. Determinant of the Jacobi matrix describes the change in the ‘volume’ during the transformation. Caustic- region where determinant of the Jacobi matrix is zero. Contrary to single lens there are regions in the plane of sky with a local minima of light that might produce drops in the brightness.
Typical separation of the two images on the sky in a single lens is 1mas (assuming M=1Msol, DS=7kpc, DL=3.5kpc) while typical resolution of a ground based telescope is 1000x worse (1as). So the images are not resolved but the magnification is observed.

Gravitational microlensing

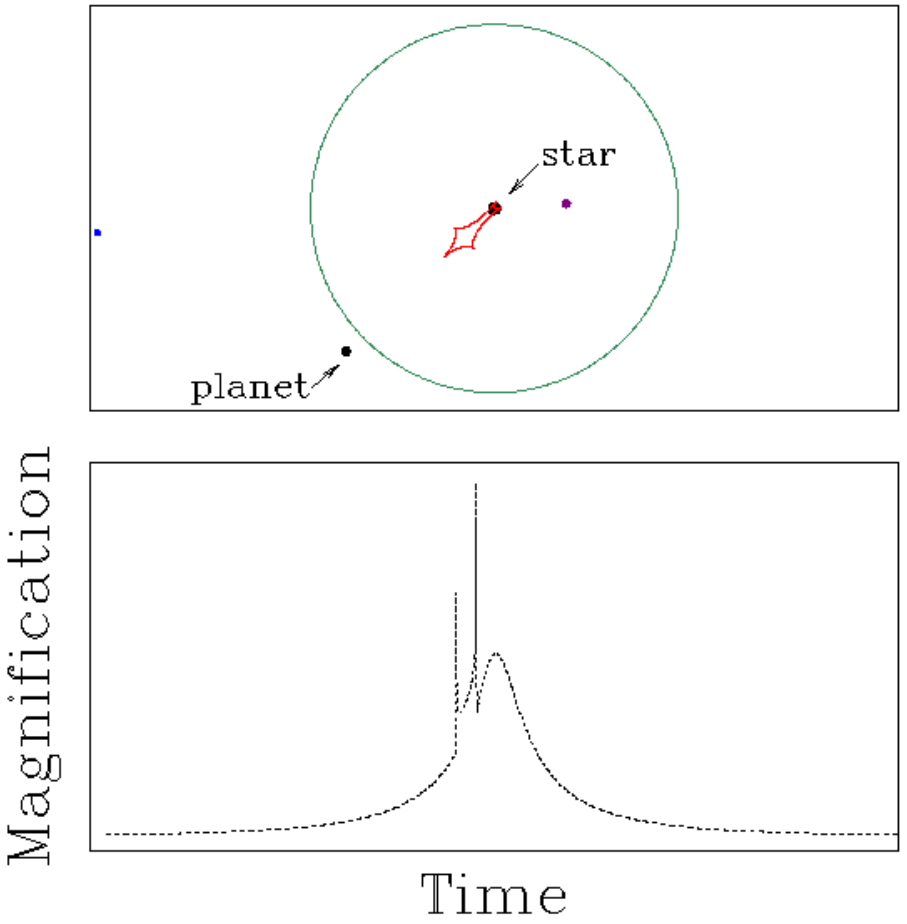

lens=star+planet are steady
Source (blue) is moving behind
Images -purple
Einstein ring -green
Caustic -red

Ogle 2003-BLG-235 first planet detection by microlensing (Bond et al. 2004).
Simulations by Scott Gaudi.

Ms=0.36Msun, Mp=1.5Mj, a=3AU (projected separation), DL=5.2kpc

Gravitational microlensing

- Creates an Einstein ring or 2 or more images which are not resolved, only a wavelength-independent symmetric amplification is observed

- OGLE project (the Optical Gravitational Lensing Experiment)

- Disadvantage: very rare event, huge number of targets, dense field- Center of Galaxy, huge and not precise distance, faint stars, problematic spectroscopic follow-up (radial velocities and orbits), event cannot be repeated

- Advantage: can get the mass ratio (from the duration of the primary and secondary peak) and projected semi-major axis, the only known ground-based method to probe earth mass planets orbiting around main sequence stars

$$\frac{m_{planet}}{m_{star}} = \frac{R_{S,p}}{R_{S,s}} = \frac{\Theta_{E,p}^2}{\Theta_{E,s}^2} = \frac{\delta t_p^2}{\delta t_s^2}$$

Imaging

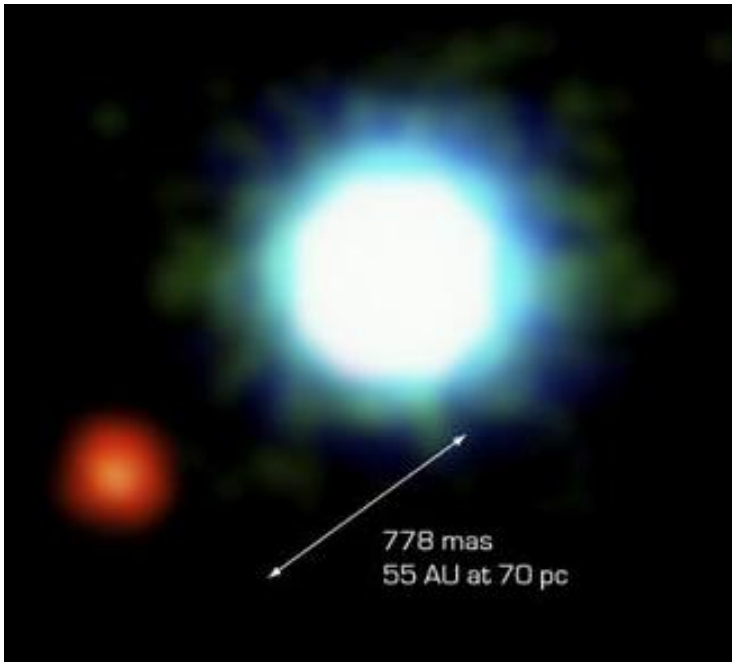

- Advantage: can get photometry, spectra, astrometry, most complete information
- Disadvantage: must cope with the glare of the star and low separation, hence bias to wide orbits, nearby and faint targets
- Adaptive optics
- Coronographs
- Interferometers (nulling)
- Visible - reflected light versus infrared-thermal emission

First image of the exoplanet 2M1207b, planetary mass companion to a young brown dwarf, 100x fainer, IR imaging with adaptive optics, VLT/NACO. It is a hot young planet shining with thermal radiation. As of IAU resolution in 2018 it may not qualify for exoplanet since its mass ratio=5 is much smaller then 25. Such object is now called a binary and its secondary is a sub-brown dwarf. Image from Chauvin et al. (2004).

Imaging

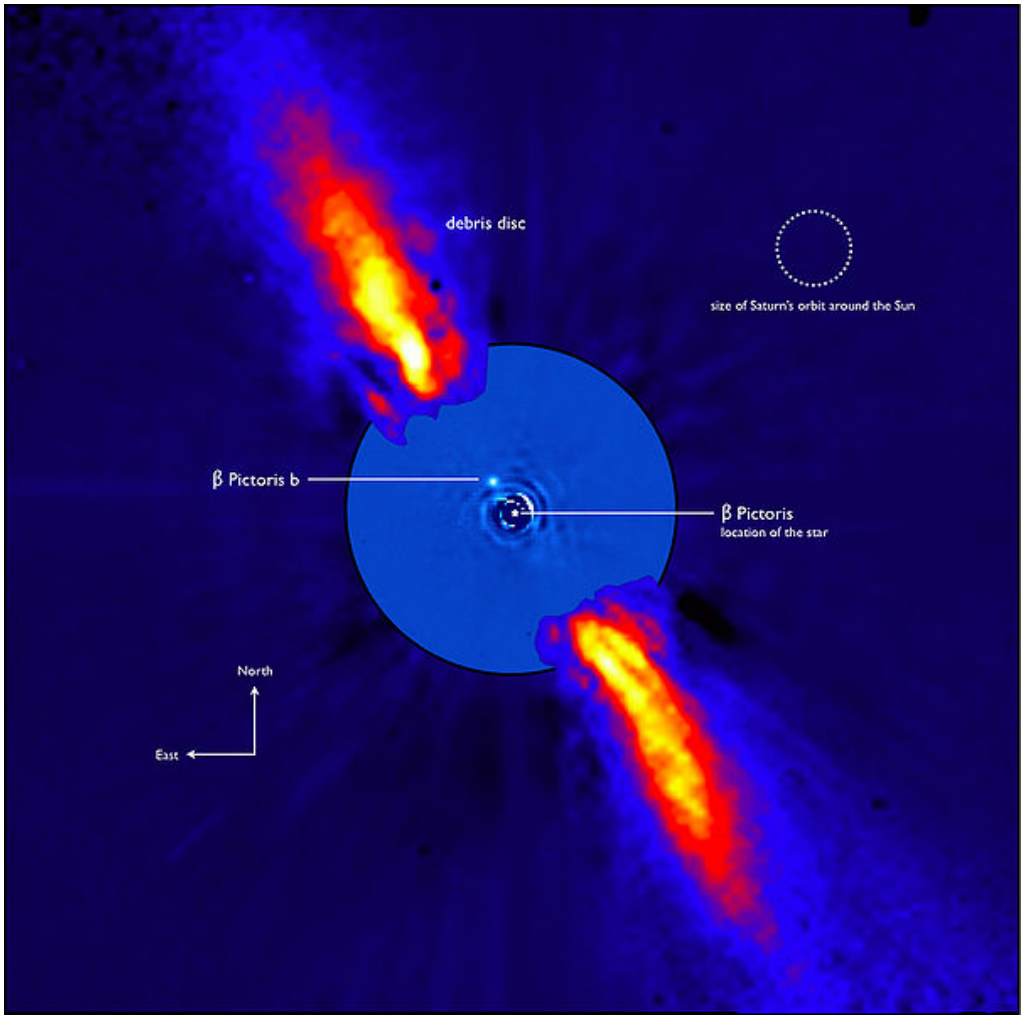

Beta Pictoris in near infrared light. ESO telescopes equipped with adaptive optics. Lagrange et al. 2009, AA, 493,L21. The faint environment is revealed after a careful subtraction of the much brighter stellar halo. The outer part of the image shows the reflected light on the dust disc, as observed in 1996 with the ADONIS instrument on ESO's 3.6 m telescope; the inner part is the innermost part of the system, as seen at 3.6 microns with NACO on the Very Large Telescope. The newly detected source is more than 1000 times fainter than Beta Pictoris, aligned with the disc, at a projected distance of 8 times the Earth-Sun distance.

Imaging

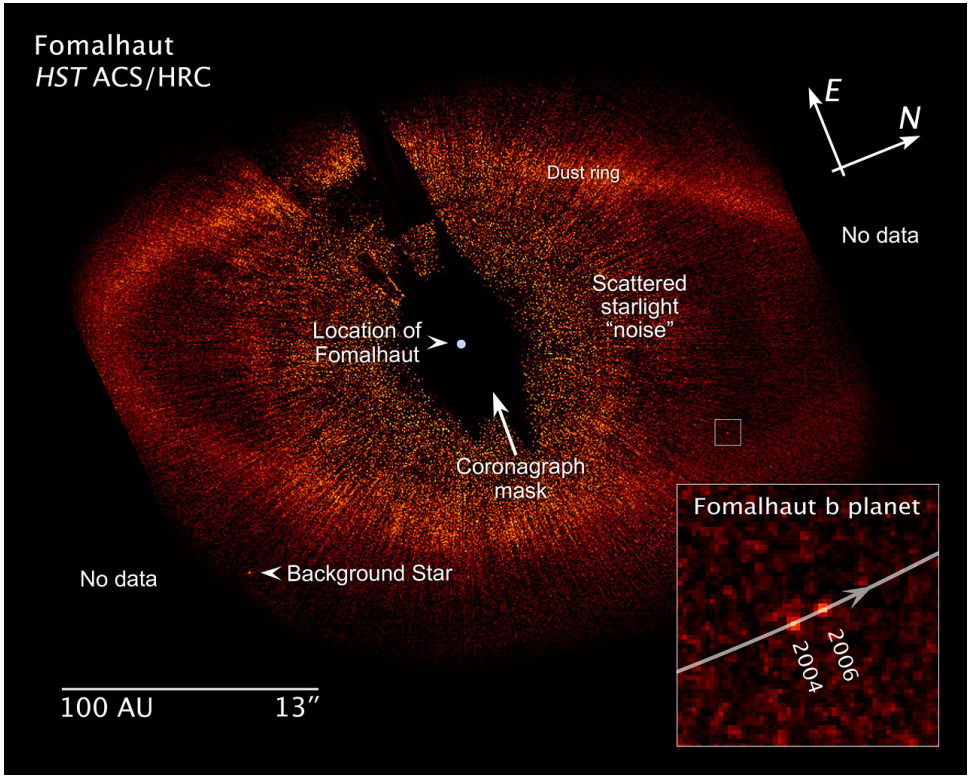

HST coronagraphic image of Fomalhaut at 0.6 µm showing the location of Fomalhaut b (white square) 12.7″ radius from the star and just within the inner boundary of the dust belt (Kalas et al. 2008, Science, 322, 5906). Or is it just the scattered light from a transient dust cloud (Janson et al.2012, ApJ, accepted)?

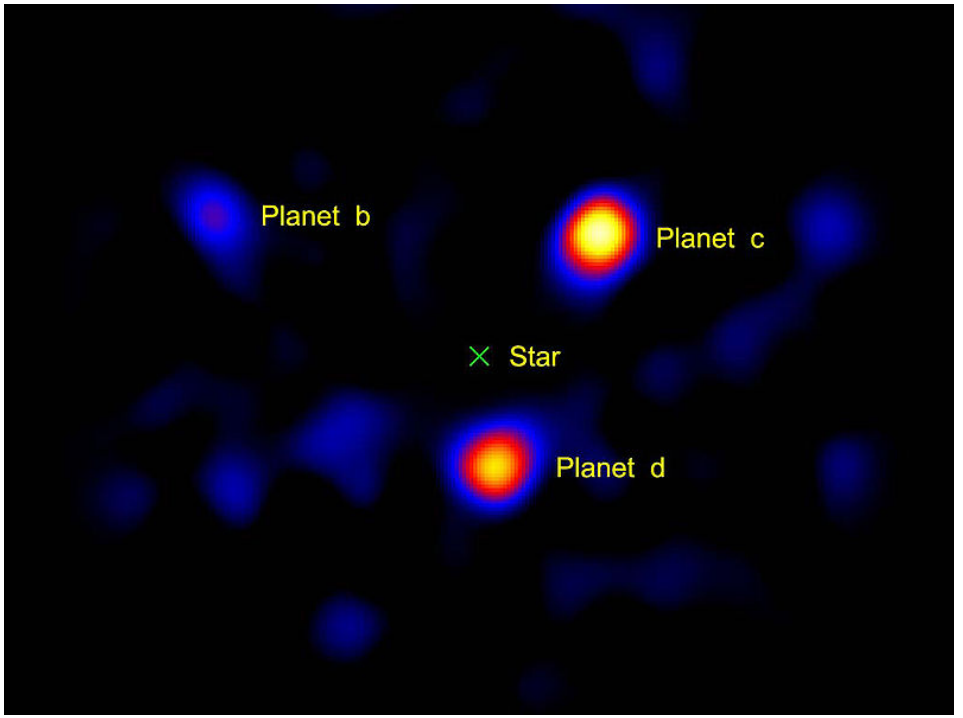

Direct image of exoplanets around the star HR8799 using a vortex coronograph on a 1.5m portion of the 5m Palomar Hale telescope. Serabyn et al. 2010, Nature, 464, 1018

Astrometry

Astrometry is the oldest astronomical method. Used for visual binaries for more than 170 yr. We do not see the planet but the star moves on an elliptical orbit around the center of mass. We measure its photo-center. It can be shown that the projection of the true elliptical orbit onto the plane of sky is an apparent orbit which is also the ellipse. The center of the true ellipse projects onto the center of the apparent ellipse. However, the focus of the true ellipse do not project onto the focus of the apparent ellipse.

There are 7 orbital elements characterizing the position of the star on its elliptical orbit: a, e, P, T, ω, Ω, i. Astrometry can determine all of them with a certain limitation.
If we do not know the distance, a-semimajor axis is only in angular units in arcseconds.
We do not know the radial velocity and whether the star is approaching or receding.
Hence, we do not know which node is ascending and which one is descending.
Hence, Ω counts from the North counterclockwise up to the first node and is within 0-180 deg. ω runs from the first node in the direction of motion up to periastron (0-360 deg).
We can determine the inclination from 1-180 deg interval. Star orbiting counterclockwise has i=0-90 deg. Star orbiting clockwise is called retrograde (i=90-180 deg). For comparison radial velocity method cannot determine the inclination and transit method only uses 0-90deg interval.

Astrometry

$$M_1 a_1 = M_2 a_2$$

Astrometric signal measured for the star -M1 is (M2-planet, d -distance to the observer):

$$\theta_1 = \frac{a_1}{d} = \frac{M_2}{M_1}\frac{a_2}{d}$$

Assuming we know the distance and the stellar mass M1 one can get the mass of the planet:

$$a^3 = P^2 (M_1 + M_2) \approx P^2 M_1, \quad M_2 = M_1 \frac{a_1}{a_2} \approx M_1 \frac{a_1}{a}$$

- Disadvantage: not precise enough at the moment but potential for the future using interferometry: GAIA (0.02 mas for 15mag), Keck (0.02mas), VLTI, long term observations, bias for close stars and face-on orbits (complementary to the spectroscopy), prone to fake variability by stellar spots

- Advantage: can get mass, detect wide companions

Star-Planet Interaction

Star interacts with the planet by definition since it orbits the star:
- Gravity => planet orbit
- Tides => synchronization, circularization, migration, shape of the planet, heating
- Stellar evolution => mainly during AGB phase: planet engulfment, destabilization of planetary orbits
- Irradiation => surface temperature, interior cooling evolution, evaporation, habitability
- Stellar wind => aurora but as a radio emission, so far only observed in Solar system planets in UV
- Light echo reflected off an exoplanet caused by stellar flares, M dwarfs, not observed yet

However, can planet affect the star?
- Tides => ellipsoidal variation in photometric signal from the star. P=Porb/2
- Star-Planet Magnetic interaction (SPMI) magnetic fields are important for habitability and planet interior

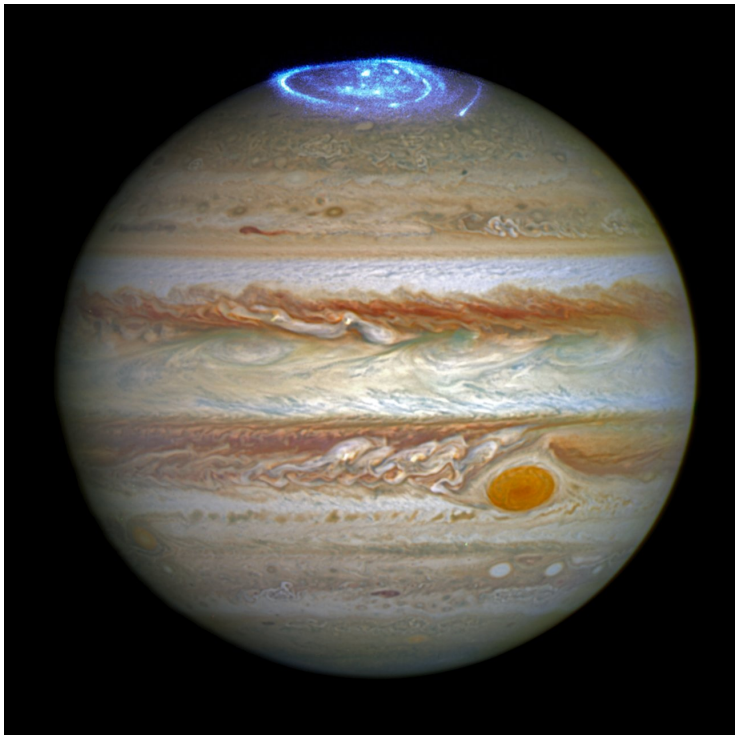

HST image of aurora on Jupiter in 2016 in UV combined with visual image. Credit: NASA, ESA

Star-Planet magnetic interaction

A few planet host stars were discovered to exhibit a star-planet magnetic interaction (SPMI) (Shkolnik et al. 2003).

Variability is observed mainly in the cores of strong lines formed high in the stellar chromosphere where magnetic energy density becomes comparable to the thermal energy density. Is variable with the orbital period of the planet.

Heating due to (1) magnetic reconnection or (2) stretching magnetic footprint at the stellar surface or (3) Alfven waves.

It suggests mag.field of hot Jupiters 20-120G (Earth=0.2-0.7G, Jupiter=4G, magnet on refrigerator=100G, MRI=10^4G) Cauley et al. 2019

Disadvantage: no planet detected, only a follow up observations, bias for close in planets, prone to fake variability by stellar spots

Advantage: can estimate magnetic fields and its interaction with the stellar magnetic fields, no need for transit

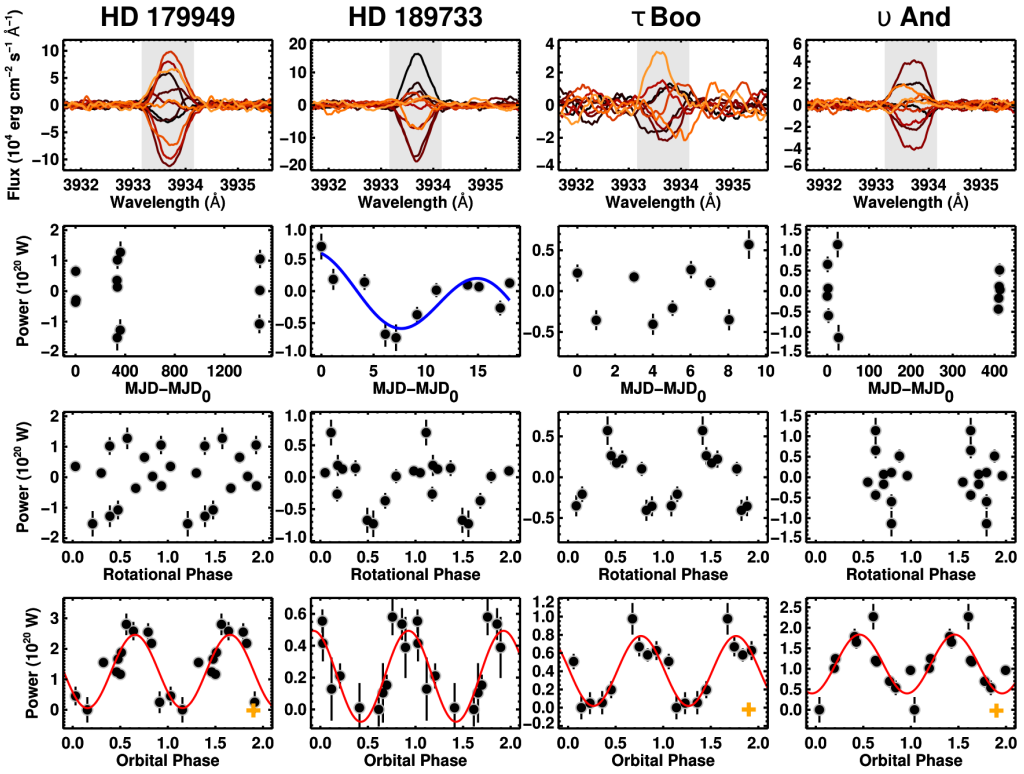

CaIIHK core variability, 1st raw spectrum residuals, raw 2-4 power as function of date or phase, Cauley et al. 2019

Rossiter-McLaughlin effect

The planetary transit affects not only the light curve but also the shape of the spectral lines and causes an asymmetry of the stellar lines. This affects the measured radial velocities. This effect can be used to study the spin-orbit alignment called the **stellar obliquity**. One can determine: impact parameter (beta) and angle between the sky projections of the planet orbital axis and stellar rotation axis (lambda).

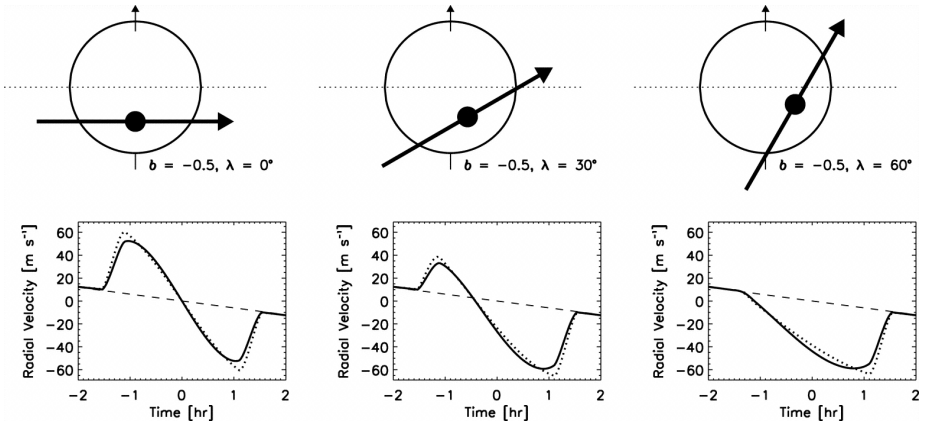

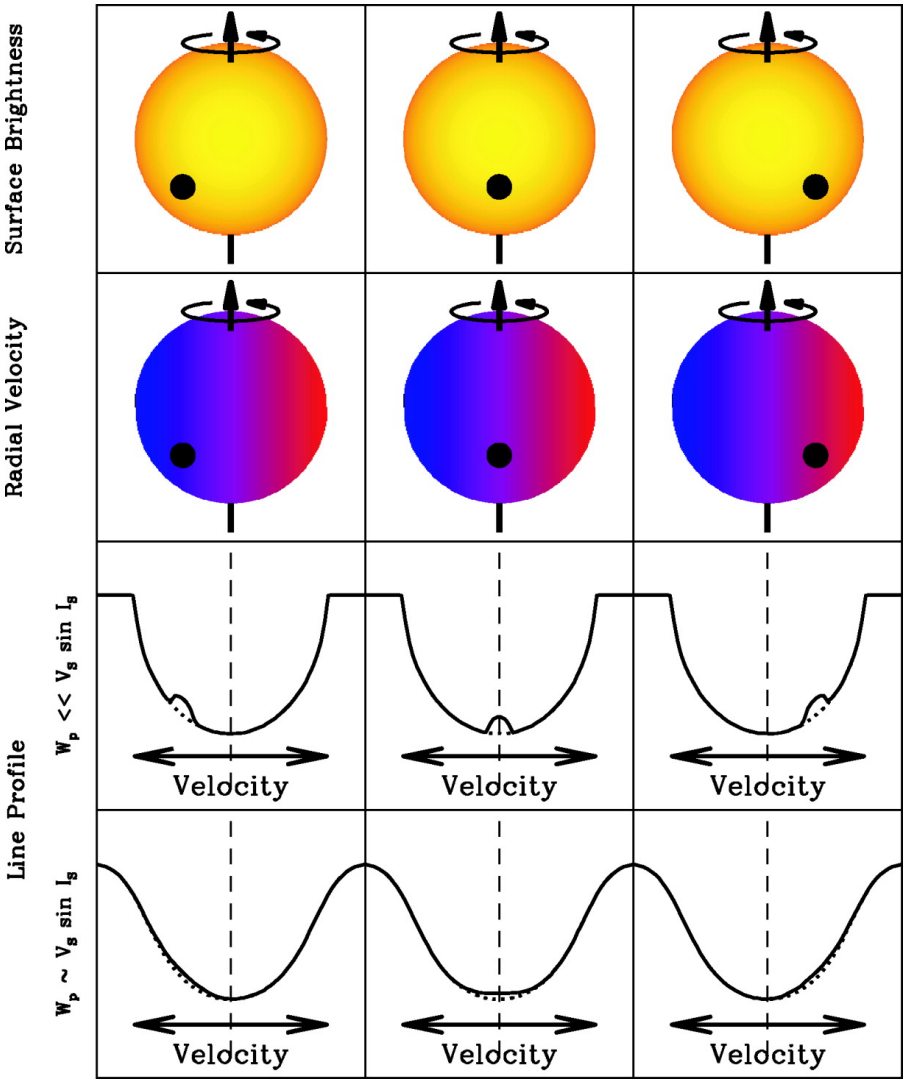

Pictures from Gaudi & Winn, 2007, ApJ 655, 550

Sensitivity of various methods